

# Rigorous investigations of Ikeda map by means of interval arithmetic

**Zbigniew Galias**

Department of Electrical Engineering, University of Mining and Metallurgy  
al. Mickiewicza 30, 30-059 Kraków, Poland  
e-mail: galias@agh.edu.pl

**Abstract.** In this work we present various tools for studying dynamical systems implemented in interval arithmetic. The methods include an algorithm for finding all low-period cycles enclosed in a specified region, finding an upper bound of the invariant and nonwandering part of a given set, finding a lower bound of the basin of attraction of a stable periodic orbit, and proving the existence of symbolic dynamics of a given type embedded in the map. Using these techniques a detailed study of the behavior of the Ikeda map for different parameter values is performed.

AMS classification scheme numbers: 37E30, 37B10, 37B40, 37C25

Submitted to: *Nonlinearity*

## 1. Introduction

Basic tools for the investigations of nonlinear systems are laboratory experiments and simulations. In simulations periodic orbits are usually found using some version of the Newton method, complex trajectories are observed by simply iterating the map on a computer in machine precision. Many of these results are left without a rigorous proof. There is no guarantee that there exist a true trajectory, which stays near the one generated by a computer. For chaotic systems, which exhibit sensitive dependence on initial conditions this problem is especially important. When we iterate the map using a computer the inevitable rounding errors cause that the trajectory generated by a computer and the true one diverge exponentially and after a certain number of iterations become uncorrelated. The question that arises is whether numerical studies of nonlinear systems are reliable at all.

In this paper we show that one can use a computer to obtain rigorous results. We present a set of tools, which can be successfully implemented to rigorously investigate nonlinear systems. The rigor is achieved by employing interval arithmetic.

We describe methods for finding all low period cycles, finding an upper bound of the invariant and nonwandering part of a given set, finding a lower bound of a basin of attraction of stable periodic orbits, methods for proving the existence of symbolic dynamics embedded within the system and obtaining lower bounds for the topological entropy of the system.

Rigorous methods for investigations of dynamical systems have been a subject of many papers. Some of the methods and algorithms used in this work has already been presented before by various authors. Below, we give references to some of the relevant papers.

Usually for the problem of finding periodic orbits of a given map  $f$ , or equivalently fixed points of  $f^n(x) - x$  one chooses a number of initial points and applies a classical iteration scheme, like Newton method. It is however uncertain whether all periodic orbits are found. We will show that methods based on interval arithmetic, when implemented properly are capable of finding all periodic orbits of considerably large periods.

Other ways of attacking this problem are also possible. In [4] a fast method for finding periodic orbits up to periods limited by the computer precision is presented. Although the method is non-rigorous in many cases it is capable of finding all orbits. Another methods for locating all zeros are based on adaptive refinement of the region of interest into smaller subsets, where the set of zeros is approximated by outer coverings [7].

Algorithms for finding upper bounds for invariant and chain recurrent of nonwandering parts of a given set are very simple and were described in many papers. A combinatorial procedure for finding an invariant part, isolating neighborhoods and index pairs is presented in [19]. A method of construction of a finite approximation of a dynamical system and a simple algorithm for localization of chain recurrent set is given

in [17]. Subdivision techniques for computation of invariant sets, invariant measures and unstable manifolds and given in [5, 6]. In all these algorithms a certain region of the state space, where we want to capture the dynamics of the system is divided into boxes (sometimes called cells). For each box a set of boxes to which a trajectory can go from a given box is found. This information is later used for obtaining an upper bound of invariant sets. For the method to be rigorous we need a way of ensuring that an enclosure of the image of a box is found. In [5] the procedure is not fully rigorous since for the computation of the image of a box a finite number of test points is used (another problem is using a non-rigorous integration procedure). This method may be made rigorous by using the information on local Lipschitz constants. For continuous time systems in order to obtain rigorous results one has to use rigorous integration methods (see [2]).

In this work we use a simpler approach based on interval computations. The image of a box is computed in one step by evaluation the map definition on the interval vector representing the box. All the computations are done in interval arithmetic and the result is an interval vector containing the image of a box.

Another approach which may be used for obtaining a global view of the behavior of a system is the method of a simple or a generalized cell mapping [12]. Once the dynamics of the system is cast in the form of mapping between cells (boxes), simple algorithms are used to extract the system behavior. A simple cell mapping is formed by dividing the region of interest into a finite number of cells. Each cell is mapped into exactly one cell, which for the purpose of analyzing of dynamical systems is chosen as the cell containing the image of the center. This method lets us investigate the approximate behavior of the system. In a generalized cell mapping a given cell is allowed to have several image cells. To each image cell a probability of going into this cell is assigned. This approach leads in a natural way to Markov chains, which may be studied in order to extract dynamical properties of the system. In most cases it is however impossible to get exact values for transition probabilities and hence the method cannot be used directly for rigorous investigations of the system.

It is difficult to rigorously estimate the topological entropy of a given map. This is a consequence of a fact that standard definitions of topological entropy using open coverings or  $\varepsilon$ -separated sets are not suited for designing rigorous numerical procedures. Most of the rigorous methods deal with one-dimensional maps. Some non-rigorous methods for higher dimensions are extensions of methods for one-dimensional systems [16]. Other non-rigorous approaches are based on counting the number of periodic points of a given period and construction of approximations of Markov partitions. In [8] a rigorous computation method of an upper bound of topological entropy of a map with respect to a finite partition is given. It is however difficult to conclude from this results something about the topological entropy of the map.

In this paper we present a method for obtaining rigorous lower bound for topological entropy based on construction of symbolic dynamics embedded within the system. The sets on which the symbolic dynamics is defined are chosen based on the structure of

nonwandering part of a subset of state space. Using finer division one can easily find more complex symbolic dynamics leading to larger bound for topological entropy.

The paper is organized as follows. In Sec. 2 several interval arithmetic methods are presented. We recall the definition of the Krawczyk operator and describe how to use it for proving the existence of periodic orbits and to find all low-period cycles of the map. We describe an algorithm for finding an upper-bound for the invariant and nonwandering part of a given set and a lower-bound for the basin of attraction of a given stable periodic orbit. We also describe a method how to prove the existence of a symbolic dynamics embedded within the map. In Sec. 3 using these methods we investigate the Ikeda map. For different parameter values we find all low-period cycles, locate the invariant and nonwandering part of the trapping region, find rigorous approximations to the basin of attraction of stable periodic orbits, prove the existence of symbolic dynamics of certain types and find estimates for the topological entropy.

## 2. Interval Tools

In this section we present various methods, which can be used for rigorous investigation of discrete dynamical systems. They share one property. All of them may be implemented in computer interval arithmetic, which allows to obtain rigorous results using a computer. Interval arithmetics is a method of computing intervals containing the true values. An excellent introduction to the interval arithmetic underlying these methods can be found in [14] or [2]. Interval arithmetic deals with closed intervals of the form  $[a, b]$ . On the set of intervals all basic arithmetic operations are defined in such a way that the result of a single operation is an interval containing all possible results. For example the sum of two intervals is defined as:

$$[a, b] + [c, d] = \{x = x_1 + x_2: x_1 \in [a, b], x_2 \in [c, d]\} = [a + c, b + d]$$

Interval arithmetic is implemented rigorously on a computer by changing the rounding modes of single operations in such a way that the computed result includes the machine precision results and the true result (computed in infinite precision). For example, when the sum of two intervals is computed the left endpoint (the operation  $a + c$ ) is evaluated in the downward rounding mode, while the right endpoint (the operation  $b + d$ ) is evaluated in the upward rounding mode.

In the following we use bold face to denote intervals, interval vectors and interval matrices and math italic to denote real quantities. We start with the description of the interval method, which allows to prove the existence of periodic orbits.

### 2.1. Existence and uniqueness of periodic orbits

Let us first recall the definition of the Krawczyk operator [15], which can be used to prove the existence and uniqueness of zeros of an  $m$ -dimensional map. Let us consider a continuously differentiable map  $f: \mathbb{R}^m \mapsto \mathbb{R}^m$ . The *Krawczyk operator* is defined as

$$\mathbf{K}(\mathbf{x}) = x_0 - Cf(x_0) - (Cf'(\mathbf{x}) - I)(\mathbf{x} - x_0), \quad (1)$$

where  $x_0$  is an arbitrary point belonging to the interval vector  $\mathbf{x}$  (usually one uses the center of  $\mathbf{x}$ ) and  $C$  is a preconditioning matrix. It is usually chosen as the inverse of  $f'(x_0)$ .

The Krawczyk operator is a version of the interval Newton operator [15, 1]  $\mathbf{N}(\mathbf{x}) = x_0 - (f'(\mathbf{x}))^{-1}f(x_0)$ . The main modification, when compared with the interval Newton operator is the introduction of a preconditioning matrix. In consequence, one does not need to compute the inverse of interval matrix and the Krawczyk operator can be used for a wider class of systems.

The following theorem [15] can be used to prove the existence and uniqueness of zeros of  $f$ .

**Theorem 1.** *If  $\mathbf{K}(\mathbf{x}) \subset \mathbf{x}$  then  $f(x) = 0$  has a unique solution in  $\mathbf{x}$  (and also in  $\mathbf{K}(\mathbf{x})$ ). If  $\mathbf{K}(\mathbf{x}) \cap \mathbf{x} = \emptyset$  then there are no zeros of  $f$  in  $\mathbf{x}$ .*

In order to prove the existence of a zero of  $f$  in  $\mathbf{x}$ , one evaluates  $\mathbf{K}(\mathbf{x})$  in interval arithmetic and checks if it is enclosed in  $\mathbf{x}$ . If this is the case the existence of a unique zero of  $f$  within  $\mathbf{x}$  is guaranteed. In order to prove that there are no zeros of  $f$  within  $\mathbf{x}$ , it suffices to show that the intersection of  $\mathbf{K}(\mathbf{x})$  and  $\mathbf{x}$  is empty. Since in interval arithmetic one can easily find the enclosure of  $\mathbf{K}(\mathbf{x})$ , the assumptions of the above theorem can be checked rigorously.

Krawczyk operator can be used for proving the existence of a period- $n$  cycle of  $f$  by applying it to the map  $g = \text{id} - f^n$ . The better choice however is to introduce a map  $F : (\mathbb{R}^m)^n \mapsto (\mathbb{R}^m)^n$  defined by

$$[F(z)]_k = x_{(k+1) \bmod n} - f(x_k) \quad (2)$$

for  $k = 0, \dots, n-1$ , where  $z = (x_0, \dots, x_{n-1})$ . Zeros of  $F$  correspond to fixed points of  $f^n$ . Using higher dimensional map  $F$  allows to deal with longer periodic orbits.

## 2.2. All periodic orbits of length $n$

In order to find all period- $n$  cycles of  $f$  in the region  $\Omega$ , we use the combination of the generalized bisection (see [13, 7]) and the Krawczyk method described above.

At the beginning the set  $\Omega$  is covered by boxes ( $m$ -dimensional interval vectors). For each interval vector  $\mathbf{x}$  we produce the sequence  $(\mathbf{x}_i)_{i=0}^{n-1}$ , where  $\mathbf{x}_i = f^i(\mathbf{x})$ , set  $\mathbf{z} = (\mathbf{x}_0, \dots, \mathbf{x}_{n-1})$ , and then the interval operator  $\mathbf{K}(\mathbf{z})$  is evaluated. Finally, we use the Theorem 1 to prove that there is exactly one fixed point of  $f^n$  in  $\mathbf{x}$  (if the assumption of the first part holds) or that there are no fixed points of  $f^n$  in  $\mathbf{x}$  (if the assumption of the second part holds). If none of these two assumptions is fulfilled the interval vector  $\mathbf{x}$  is divided into smaller parts and the computations are repeated. Below we describe this algorithm in terms of a simple model language.

```
procedure FindPeriodicOrbitsInBox( $\mathbf{x}$ )
```

```
   $\mathbf{x}_0 \leftarrow \mathbf{x}$ ;
```

```
  for  $i \in \{1, \dots, N-1\}$  do begin
```

```

     $\mathbf{x}_i \leftarrow f(\mathbf{x}_{i-1});$ 
end
 $\mathbf{z} \leftarrow (\mathbf{x}_0, \mathbf{x}_1, \dots, \mathbf{x}_{n-1}),$ 
compute  $\mathbf{K}(\mathbf{z});$ 
if  $\mathbf{K}(\mathbf{z}) \subset \mathbf{z}$  then begin
     $Q \leftarrow Q + 1;$ 
    record  $\mathbf{x};$ 
    return;
end
if  $\mathbf{K}(\mathbf{z}) \cap \mathbf{z} = \emptyset$  then begin
    return;
end
divide  $\mathbf{x}$  into  $\mathbf{y}_1, \dots, \mathbf{y}_{2^m};$ 
for  $i \in \{1, \dots, 2^m\}$  do begin
    FindPeriodicOrbitsInBox( $\mathbf{y}_i$ );
end
end of FindPeriodicOrbitsInBox

```

$Q$  is a global variable, which at the beginning of computations is initialized to be zero, and at the end is equal to the number of fixed points of  $f^n$  in the region considered.

Observe, that the version of the bisection algorithm presented here is different from the one usually used. In a typical implementation of generalized bisection for finding all zeros of the map  $F$  defined by equation (2) the division is performed on the box  $\mathbf{z}$ . This means that in order to find all period- $n$  orbits of an  $m$ -dimensional map we are searching the  $mn$ -dimensional space. Simulations show that this choice is very inefficient and that making divisions in the original space (dividing  $\mathbf{x}$  and then generating  $\mathbf{z}$ ) leads to a much faster algorithm.

We can further speed up the algorithm utilizing the fact that we are searching for periodic orbits. For the interval vector  $\mathbf{x}$  we compute several forward and backward (the Ikeda map is invertible) iterates  $f^i(\mathbf{x})$ . First, if any of these iterates has empty intersection with  $\Omega$  then  $\mathbf{x}$  does not contain a periodic point, for which the whole orbit is enclosed in  $\Omega$ . Second, if any of these iterates is enclosed in the region for which the algorithm was completed then there are no new periodic orbits in  $\mathbf{x}$ . In both cases we can skip the interval  $\mathbf{x}$ .

Using the algorithm and the modifications presented above one can find all period- $n$  orbits for a considerably large  $n$ .

Once the box enclosing the the periodic point  $\bar{x}$  is found, we can find very narrow enclosure of its position by iterating the Krawczyk operator ( $\bar{x} \in \mathbf{K}(\mathbf{x}) \subset \mathbf{x}$ ). We can also find an enclosure of the Jacobian matrix of  $f^n$  at the periodic point and decide the stability of the orbit. In rare cases it may happen that the computed enclosure of one of the eigenvalues contains a number with absolute value equal to 1. In such a case, we are not sure what is the stability type.

### 2.3. Invariant and nonwandering part

In this section we present a method for finding an upper bound for invariant part and nonwandering part of a given set. Invariant and nonwandering components are important in the study of dynamical systems. They represent stationary or repeatable behavior.

The *invariant part* of a set  $\Omega$  under action of  $f$  is defined as

$$\text{Inv}(\Omega) = \{x: \exists (x_k)_{k=-\infty}^{\infty} \text{ such that } x_0 = x, x_k \in \Omega \text{ and } x_{k+1} = f(x_k)\}. \quad (3)$$

A point  $x$  is called *nonwandering* for the map  $f$  if for any neighborhood  $U$  of  $x$  there exists  $n > 0$  such that  $f^n(U) \cap U \neq \emptyset$ . For a given set  $\Omega$  we define the *nonwandering part* of  $\Omega$  as the set of nonwandering points of the map  $f|_{\text{Inv}(\Omega)}$ . The set of nonwandering points is closed and it contains the closure of the set of fixed points and periodic orbits.

Now we describe an algorithm for finding the enclosure of the invariant part [19, 5] and nonwandering part of a set. The enclosure found will be the union of  $\varepsilon$ -boxes, i.e. sets of the form

$$\mathbf{v} = [k_1\varepsilon_1, (k_1 + 1)\varepsilon_1] \times [k_2\varepsilon_2, (k_2 + 1)\varepsilon_2] \times \cdots \times [k_m\varepsilon_m, (k_m + 1)\varepsilon_m], \quad (4)$$

where  $k_i$  are integer numbers,  $\varepsilon_i$  for  $i = 1, 2, \dots, m$  are fixed positive real numbers, and  $\varepsilon = (\varepsilon_1, \varepsilon_2, \dots, \varepsilon_m)$ . For a set of boxes  $V = \{\mathbf{v}_i\}$ , by  $|V|$  we will denote the sum of all boxes in  $V$  ( $|V| = \bigcup \mathbf{v}_i$ ).

In order to find the invariant part of a given set  $\Omega$ , we first cover  $\Omega$  by  $\varepsilon$ -boxes. The set of boxes  $V = \{\mathbf{v}_i\}$  serves as a covering of  $\text{Inv}(\Omega)$ . Next, the set  $E$  of possible transitions between boxes is generated.

$$E = \{(i, j): f(\mathbf{v}_i) \cap \mathbf{v}_j \neq \emptyset\}.$$

If  $(i, j) \notin E$  then a trajectory after being in  $\mathbf{v}_i$  cannot go to  $\mathbf{v}_j$ . In the course of the procedure the set  $V$  is decreased by removing boxes which lie outside the invariant part. The box  $\mathbf{v}_i$  is removed from the set  $V$  if its image has empty intersection with  $V$  (i.e.,  $f(\mathbf{v}_i) \cap V = \emptyset$  or equivalently  $\forall j (i, j) \notin E$ ) or if it has empty intersection with the image of  $V$  (i.e.,  $\mathbf{v}_i \cap f(V) = \emptyset$  or equivalently  $\forall j (j, i) \notin E$ ). This procedure is continued until no more boxes can be removed. The remaining boxes are an upper bound of the invariant part of  $\Omega$ .

procedure FindInvariantPart( $V$ )

$E \leftarrow$  the set of possible transitions ( $(i, j) \in E$  if  $f(\mathbf{v}_i) \cap \mathbf{v}_j \neq \emptyset$ );

repeat

  Done  $\leftarrow$  TRUE;

  for all  $\mathbf{v}_i \in V$  do begin

    if  $\forall j (i, j) \notin E$  or  $\forall j (j, i) \notin E$  then begin

      remove  $\mathbf{v}_i$  from  $V$ ;

$\forall k$  remove  $(i, k)$  and  $(k, i)$  from  $E$ ;

      Done  $\leftarrow$  FALSE;

    end

```

end
until not Done;
end of FindInvariantPart

```

The most time consuming part of the algorithm is the generation of the set of admissible transitions  $E$ . Since the computations are done in interval arithmetic, the found set  $E$  is the enclosure of the set of admissible transitions. In order to obtain a possibly narrow enclosure the set  $f(\mathbf{v}_i)$  has to be found using a standard technique of decomposing  $\mathbf{v}_i$  into several smaller boxes and finding their images under  $f$  individually.

The above procedure is stopped, when no more boxes can be removed. The obtained set  $|V|$  is the best enclosure one can obtain for a given precision of dividing the state space into boxes. We can easily obtain a better upper bound of the invariant part by refining the division of  $V$  and calling the procedure `FindInvariantPart` again.

Nonwandering part may be smaller than the invariant part. For example the nonwandering part does not contain a heteroclinic connection connecting unstable fixed point and attracting fixed point, since all trajectories from a sufficiently small neighborhood of the heteroclinic orbit converge to the attracting fixed point. An example for the Ikeda map will be shown in section 3.

Let us observe that if a box  $\mathbf{v}_i$  contains nonwandering points then there must exist a closed sequence of boxes  $(\mathbf{v}_{i_1}, \mathbf{v}_{i_2}, \dots, \mathbf{v}_{i_k})$  such that  $i = i_1 = i_k$  and  $f(\mathbf{v}_{i_j}) \cap \mathbf{v}_{i_{j+1}} \neq \emptyset$  for  $j = 1, 2, \dots, k - 1$ . Hence, when finding an upper bound of the nonwandering part we additionally remove boxes, for which there is no closed sequence of boxes passing through it. The problem of finding such boxes can be reduced to decomposition of the graph (where boxes define vertices and elements of the set  $E$  define edges) into strongly connected components (compare also [6]). This is a standard problem in algorithmic graph theory and has a very fast solution, which operates in a linear time [10]. Strongly connected components consisting of a single vertex  $v_i$ , such that  $(i, i) \notin E$  correspond to boxes, which should be removed.

The procedure for finding the nonwandering part is basically the same as the procedure `FindInvariantPart`. The only modification is removing the box  $\mathbf{v}_i$  from  $V$  also if the box  $\mathbf{v}_i$  does not belong to any closed loop.

Studying of invariant part and nonwandering part of a given set is a very important problem in theory of dynamical systems and the procedures presented above give very good enclosures of these sets, as shown in the Section 3. The enclosure for invariant or nonwandering components can also be helpful in finding periodic orbits. Since nonwandering part of  $\Omega$  contains all periodic orbits enclosed in  $\Omega$  it is clear that in the search for periodic orbits we can limit ourselves to the invariant part or even better the nonwandering part. It is possible to further explore the structure of closed loops of boxes in the graph used for removing boxes containing only wandering points. In order to find all period- $n$  orbits it is enough to generate all closed loops of boxes of length  $n$  and check these boxes. This improvement allows us to construct a very fast algorithm for finding all period- $n$  cycles.

The knowledge about nonwandering and invariant part of the trapping region together with the position of fixed and periodic points and their basins of attraction (see next section) let us study the structure of stable and unstable manifolds, homoclinic and heteroclinic connections. Examples are shown in Section 3.

#### 2.4. Basin of attraction of a stable periodic orbit

Basin of attraction of an asymptotically stable periodic orbit  $p$ , with a neighborhood  $U$  of points converging to  $p$  is defined as the set of points, which eventually go into  $U$ . Here we are interested in finding a possibly large subset  $B$  of a given set  $\Omega$ , such that  $B$  is enclosed in the basin of attraction of  $p$ .

In order to perform this task, we first find a neighborhood  $U$  of the the orbit  $p$ , which is mapped into itself, such that trajectories of points in  $U$  converge to the periodic orbit. This can always be done since by assumption the orbit is asymptotically stable.

Then we cover the region  $\Omega$  by  $\varepsilon$ -boxes of a given size. We split the covering into two parts. The first part  $V$  is initially empty. The remaining boxes define the second part  $W$ . During the procedure, the box is moved from the set  $W$  to  $V$  if the box itself or its image is enclosed in  $U \cup |V|$ . Since at the beginning  $V$  is empty we initially transfer boxes, which are enclosed in  $U$ . Then  $V$  becomes larger and more and more boxes can be moved from  $W$  to  $V$ . The process is continued until  $V$  cannot be increased.

It is clear that any trajectory starting in  $|V|$  converges to the stable periodic orbit considered. The set of boxes  $V$  gives us a lower bound of the basin of attraction of the periodic orbit  $p$ . The accuracy of the representation depends on the size of boxes which are used for covering. In order to get a better lower bound we refine the division of  $W$  and repeat the computations. Decreasing  $\varepsilon$  is continued until a final accuracy  $\delta$  is achieved.

The procedure for finding a subset of  $\Omega$  of points, which eventually visit  $U$  is presented below.

```

procedure FindBasin( $U, \Omega, V$ )
   $V \leftarrow \emptyset$ ;
   $W \leftarrow$  the set of  $\varepsilon$ -boxes covering  $\Omega$ ;
  repeat
    repeat
      Done  $\leftarrow$  TRUE;
      for all  $\mathbf{w}_i \in W$  do begin
        if  $\mathbf{w}_i \subset U \cup |V|$  or  $f(\mathbf{w}_i) \subset U \cup |V|$  then
          move  $\mathbf{w}_i$  from  $W$  to  $V$ ;
        Done  $\leftarrow$  FALSE;
      end
    end
  until not Done;
   $\varepsilon \leftarrow \varepsilon/2$ ;

```

```

    W ← the set of  $\varepsilon$ -boxes covering W;
    until (min( $\varepsilon$ ) <  $\delta$ );
end of FindBasin

```

In Section 3 basins of attraction of stable fixed points and period–2 orbit are found. The information about basins of attraction can also be used for searching for periodic orbits. It is clear that the orbit  $p$  is the only periodic orbit enclosed within its basin of attraction. Hence, once the stable periodic orbit  $p$  is located and its basin of attraction  $B$  is found we can exclude the region  $B$  from the search space for periodic orbits of arbitrary period.

### 2.5. Proving the existence of symbolic dynamics

In this section we describe a topological method, we use to prove the existence of symbolic dynamics. The method is based on the concept of covering [20].

For simplicity, let us assume that  $f$  is a continuous two–dimensional map. For the description of covering relations in higher dimension see [20]. Let us choose  $p$  pairwise disjoint quadrangles  $N_1, N_2, \dots, N_p$ . For each  $N_i$  we choose two opposite edges and call them “horizontal”. The two others are called “vertical”. We say that  $N_i$   $f$ –covers  $N_j$  and we use the notation  $N_i \xrightarrow{f} N_j$  if

- (i) the image of  $N_i$  under  $f$  has empty intersection with the horizontal edges of  $N_j$ ,
- (ii) the images of vertical edges of  $N_i$  has empty intersection with  $N_j$  and they are located geometrically on the opposite sides of  $N_j$ .

To prove that a certain covering relation  $N_i \xrightarrow{f} N_j$  holds, we cover the edges of  $N_i$  by boxes of a specified size. Next, we find images of these boxes under  $f$  and check the conditions (i) and (ii).

Once the existence of covering relations is proved, we have the existence of symbolic dynamics, as stated by the following theorem.

**Theorem 2.** *Let  $N_1, N_2, \dots, N_p$  be pairwise disjoint quadrangles. Let  $A = (a_{i,j})_{i,j=1}^n$  be a square matrix, where*

$$a_{i,j} = \begin{cases} 1 & \text{if } N_i \xrightarrow{f} N_j, \\ 0 & \text{otherwise.} \end{cases} \quad (5)$$

*Then  $f$  is semiconjugate with the subshift on  $p$  symbols, with the transition matrix  $A$ .*

*Proof.* The semiconjugacy is a simple consequence of the existence of a trajectory realizing a given sequence of coverings (see [9], Theorem 1).  $\square$

From the fact that  $f$  is semiconjugate with a subshift of a finite type, we can make conclusions on the topological entropy of  $f$ . Topological entropy of a subshift of finite type with transition matrix  $A$  equals to the logarithm of the dominant eigenvalue  $\lambda_1$  of  $A$ , i.e.,  $\lambda_1$  is such that  $\lambda_1 \geq |\lambda_j|$  for all eigenvalues of  $A$  (see [18][Theorem 1.9,

p. 340]). The topological entropy of a map semiconjugate to a subshift is not less than the topological entropy of this subshift. Thus, we have the following result.

**Theorem 3.** *The topological entropy of the map  $f$  is not smaller than the logarithm of the dominant eigenvalue of the matrix  $A$ , defined by equation (5)*

$$H(f) \geq \log \lambda_1. \quad (6)$$

Unfortunately, according to our knowledge there is no fully automatic method for finding sets  $N_i$  on which complicated symbolic dynamics is defined. In order to find the sets  $N_i$  we use the technique based on construction of invariant or nonwandering part of a given set. First we find the nonwandering part of a given set. Usually this set is connected and it does not help us much in finding the rectangles  $N_i$ . To break this set into several pieces we remove part of this set and find the invariant part of what is left. In many cases the result is a small number of connected components, which after minor modification can serve as the rectangles  $N_i$ .

### 3. Analysis of the Ikeda map

As an example, we consider the Ikeda map [11]

$$f(z) = p + B \exp(i\kappa - i\alpha/(1 + |z|^2)) z, \quad (7)$$

where  $z = x + iy$  is a complex number. This map can be written as a two-dimensional system in the following form:

$$f(x, y) = (p + B(x \cos t - y \sin t), B(x \sin t + y \cos t)), \quad (8)$$

where  $t = t(x, y) = \kappa - \alpha/(1 + x^2 + y^2)$ .

It is known that the ball  $K = B((p, 0), pB/(1 - B))$  is a trapping region for the map  $f$  (i.e.,  $f(K) \subset K$ ) [11]. Furthermore it can be shown that the trajectory starting at arbitrary point  $(x, y) \in \mathbb{R}^2$  enters the ball  $K$  in finite time. Thus, we can limit our analysis of the behavior of the system to the region  $K$ .

We consider the Ikeda map with the following parameter values:  $p = 1$ ,  $B = 0.9$ ,  $\kappa = 0.4$  and  $\alpha = 3, 6, 7$ .

Let us start with non-rigorous numerical investigations. Computer generated trajectories starting at the origin  $(x, y) = (0, 0)$  for different parameter value  $\alpha$  are shown in Fig. 1. In the first case the trajectory converges to the fixed point. For  $\alpha = 6$  one observes a chaotic trajectory. In the last case, for  $\alpha = 7$  the trajectory initially behaves in a complex way but eventually converges to the period-2 orbit. In order to be able to say something more about the dynamics of the system one has to generate many trajectories starting in different initial conditions. This kind of analysis is rather time consuming and does not give us full knowledge of the system, even about its stable low-period cycles, not to mention unstable ones. A stable low-period cycle may have very small basin of attraction (when compared to other basins) and may be not found using this procedure and random initial conditions. For example in the case of  $\alpha = 3$  there is a second fixed point, but a chance of choosing an initial point in the rectangle

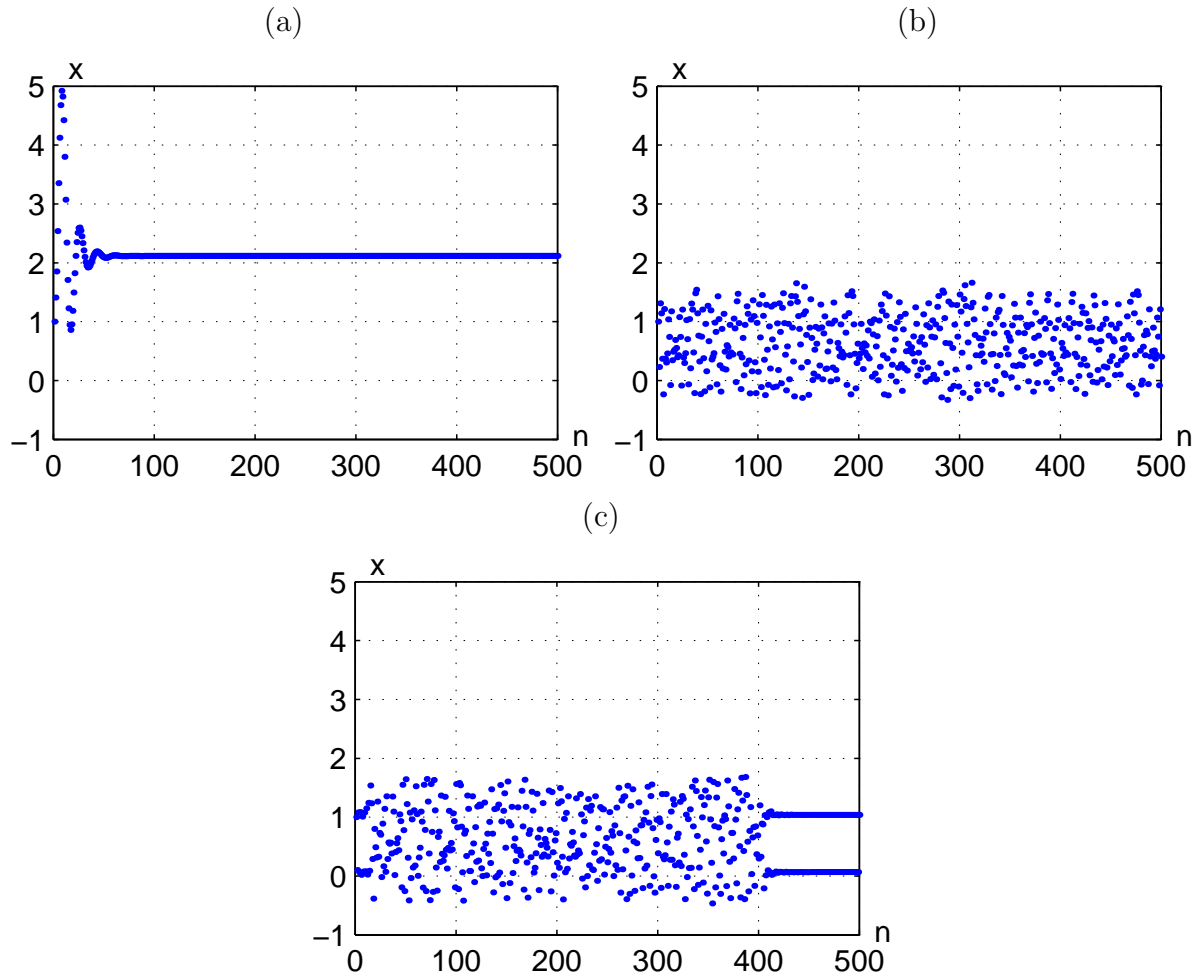


**Figure 1.** Ikeda map, computer generated trajectory of the point  $(x, y) = (0, 0)$  for (a)  $\alpha = 3$ , (b)  $\alpha = 6$  and (c)  $\alpha = 7$ .

$[-10, 10] \times [-10, 10]$  belonging to its basin of attraction is smaller than  $1/500$  (most trajectories converge to the other fixed point).

In the next sections we show that it is possible, with not much effort, to analyze the system rigorously using a computer. One can study the structure of invariant sets, find all low period cycles and basins of attraction of stable periodic orbits. One can also prove the existence of symbolic dynamics of the map and find rigorous bounds for its topological entropy.

### 3.1. Ikeda map for $\alpha = 3$

First, let us consider the case  $\alpha = 3$ . For this parameter value one observes in computer simulations the convergence of the trajectories to one of the two stable fixed points  $P_{1,2}$ . There also exists a third saddle-type fixed point  $P_3$ . The positions of these fixed points found with the Krawczyk method are following:

$$P_1 \in (2.115590405128_{69}^{72}, 3.5398435033989_{52}^{76}),$$

$$P_2 \in (0.562256442698_{598}^{603}, -0.5824076479740_{53}^{39}),$$

$$P_3 \in (0.5918772297744_{48}^{54}, -0.7853725735868_{58}^{31}).$$

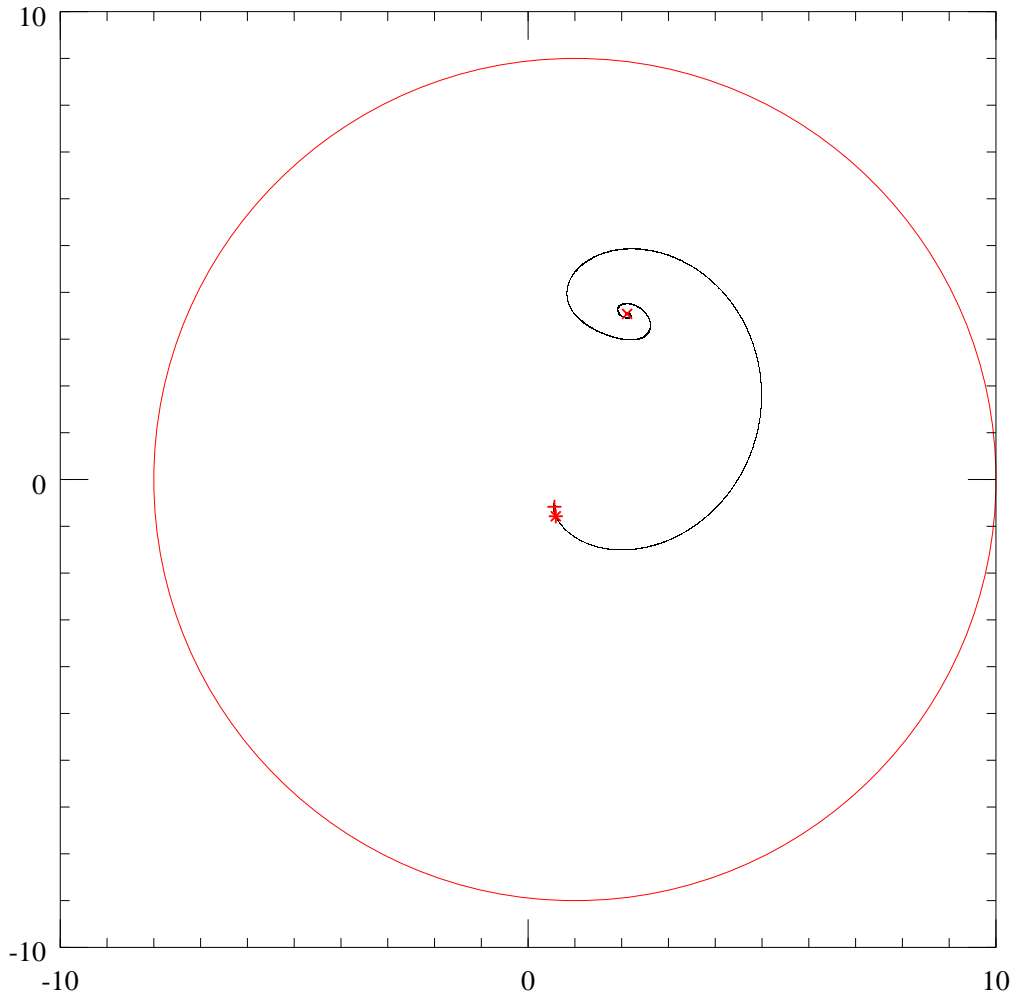


**Figure 2.** Ikeda map,  $\alpha = 3$ , invariant part of the trapping region, the stable fixed points  $P_1$  and  $P_2$  ( $\times$ ,  $+$ ), the unstable fixed point  $P_3$  ( $*$ ).

The invariant part of the trapping region  $K$ , found with the method described in Section 2.3 is shown in Fig. 2. The invariant part contains the three fixed points and the heteroclinic orbits connecting the saddle type fixed point and two stable fixed points. The area of the set of boxes containing the invariant part is 0.0465 and is very small when compared to the area of the trapping region  $K$ , which is  $\pi 9^2 \approx 254.5$ .

We have also found the upper bound of the nonwandering part of the trapping region. The area of the boxes containing the nonwandering part is smaller than  $6 \cdot 10^{-7}$ . It consists of three small regions. Each of them contains a single fixed point. Using the hyperbolicity conditions in these regions it can be shown that if the trajectory stays in one of this regions it must necessarily converge to the fixed point. Since all periodic orbits belong to the nonwandering part, it follows that there are no other periodic orbits for  $\alpha = 3$ .

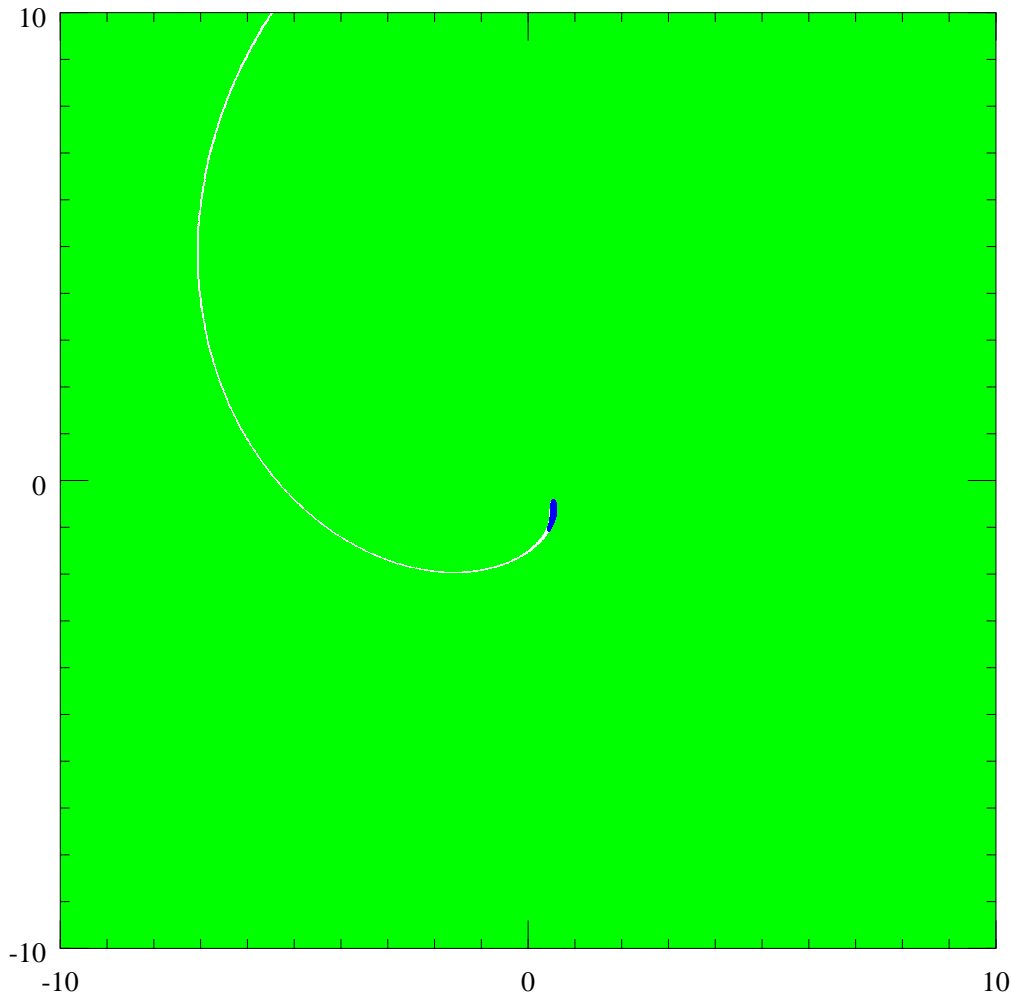


**Figure 3.** Ikeda map,  $\alpha = 3$ , basins of attraction of the stable fixed points  $P_1$  and  $P_2$ .

In order to better understand the dynamics of the system we have found basins of attraction  $B_1, B_2$  of the stable fixed points  $P_1, P_2$ . First we have located trapping regions around each of the stable fixed points. The size and the shape of the basin of attraction is a global feature and cannot be studied by means of the Jacobian matrix at the stable fixed point alone. However analysis of the Jacobian matrix helps us to choose the initial trapping region. Close to the fixed point where the linear approximation based on the Jacobian matrix is valid we may easily find a small ellipse which is a trapping region. The matrix norm induced by the Euclidean norm for the Jacobian matrices is 1.753 for the Jacobian matrix at  $P_1$  and 1.0527 for the Jacobian matrix at  $P_2$ . It means that in the linear approximation circles are not trapping regions and in order to find a good candidate we need to start with an ellipse. We have found the following ellipses which are trapping regions for the map:

$$\left( \frac{\cos^2 \varphi}{r_1^2} + \frac{\sin^2 \varphi}{r_2^2} \right) (x - x_0)^2 + \left( \frac{\sin^2 \varphi}{r_1^2} + \frac{\cos^2 \varphi}{r_2^2} \right) (y - y_0)^2 +$$

$$\left(\frac{1}{r_1^2} - \frac{1}{r_2^2}\right) \sin(2\varphi)(x - x_0)(y - y_0) \leq 1,$$

where  $x_0 = 2.11559$ ,  $y_0 = 3.53984$ ,  $r_1 = 2.3$ ,  $r_2 = 1.4$ ,  $\varphi = -0.3$  for  $P_1$  and  $x_0 = 0.562256$ ,  $y_0 = -0.582407$ ,  $r_1 = 0.03$ ,  $r_2 = 0.09$ ,  $\varphi = 0.08$  for  $P_2$ .

Then using the hyperbolicity of the fixed points we have shown that the invariant part of these trapping regions is the fixed point (all trajectories starting in the trapping regions converge to the fixed point).

Finally using the algorithm described in Section 2.4 we have found regions belonging to the basins of attraction. In Fig. 3 the basins of attraction of the stable fixed points are plotted.

Since the Ikeda map is area contracting (the determinant of the Jacobian is constant  $\det f'(x) = B^2 = 0.81$ , which means that areas contract by  $B^2$  on each iteration of the map) it is clear that each basin of attraction must have infinite area. It is interesting to observe that although the eigenvalues of the Jacobian matrix at the two stable fixed points have the same magnitude the basins are very different. Most of the points belong to the basin  $B_1$ . We have shown that from the rectangle  $[-10, 10] \times [-10, 10]$  the region with area 399.039 is enclosed in  $B_1$  and the region with area 0.075 is enclosed in  $B_2$ . The set of remaining points contains the boundary between the two basins. The boundary consists of the unstable fixed point and its stable manifold.

Summarizing, we have managed to perform the full analysis of the dynamics for the considered case. We have shown that there are only three fixed points and no other periodic orbits. We have found very good approximations of the heteroclinic connections between the fixed points. We have also found basins of attraction of the stable fixed points. Most points lie in the basin of attraction of the fixed point  $P_1$ .

### 3.2. Ikeda map for $\alpha = 6$

For  $\alpha = 6$  in simulations one observes chaotic behavior. Some trajectories converge to the stable fixed point and others display complex non-periodic oscillations.

There are three fixed points of the map. They belong to the following interval vectors:

$$\begin{aligned} P_1 &\in (2.9721316179105_{38}^{71}, 4.145946421395_{87}^{91}), \\ P_2 &\in (0.5327546229407_{88}^{93}, 0.24689677271101_{12}^{49}), \\ P_3 &\in (1.114269614581_{39}^{43}, -2.2856944609861_{69}^{45}). \end{aligned}$$

The first fixed point is stable and the two others are unstable.  $P_2$  belongs to the numerically observed chaotic attractor.

First, we have found sets of boxes enclosing the invariant part and the nonwandering part of the trapping region. The results are shown in Fig. 4 and 5 respectively.

The invariant part contains the stable fixed point, unstable fixed point  $P_3$ , the chaotic attractor observed numerically and unstable manifold of  $P_3$  connecting this point with the stable fixed point and the chaotic attractor. The area of the upper bound of the invariant part is 2.22.

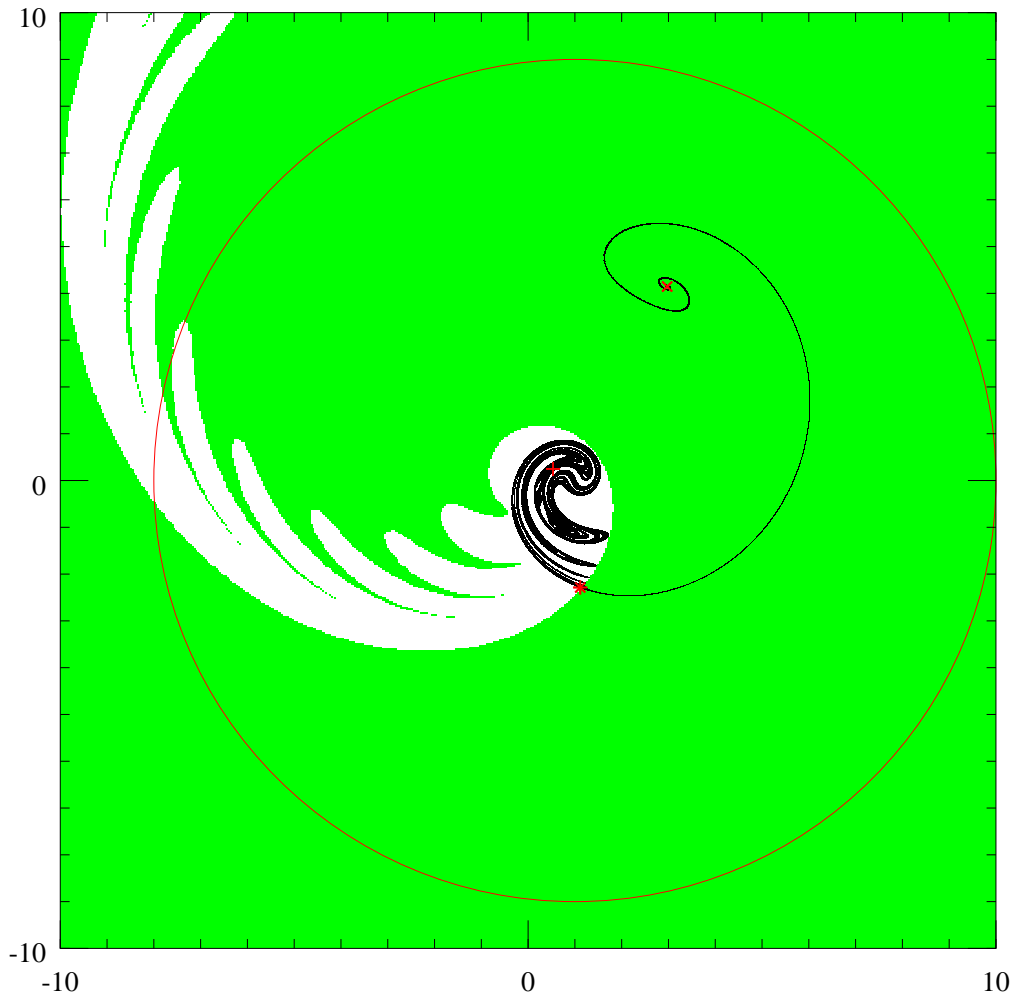


**Figure 4.** Ikeda map,  $\alpha = 6$ , the trapping region  $K$  and its invariant part (black), basin of attraction of the stable fixed point  $P_1$  ( $\times$ ), the unstable fixed points  $P_2$  and  $P_3$  ( $+$ ,  $*$ ).

The enclosure of the nonwandering part is smaller. Its area is 2.01. It does not contain the heteroclinic orbit connecting  $P_3$  and  $P_1$ . We were not able however to break the connection between  $P_3$  and the region containing the numerically observed attractor.

Next, we have found the basin of attraction of the stable fixed point  $P_1$ . In the first step we have shown that the ellipse (9) with  $x_0 = 2.972132$ ,  $y_0 = 4.145946$ ,  $r_1 = 1.2$ ,  $r_2 = 2.1$ ,  $\varphi = 1$  is a trapping region for the map and we have proved that the invariant part of this ellipse is  $P_1$  (all trajectories starting in the ellipse converge to the fixed point). Finally, we have found a subset of the rectangle  $[-10, 10] \times [-10, 10]$  enclosed in the basin of attraction of  $P_1$  (see Fig. 4). The region found has an area of 357.005.

Using the Krawczyk method, we have found all periodic orbits with period  $n \leq 15$ . Periodic orbits found (apart from the stable fixed point  $P_1$ ) are shown in Fig 6. One can see that low-period cycles do not fill the attractor uniformly and an interesting Cantor set structure is formed.

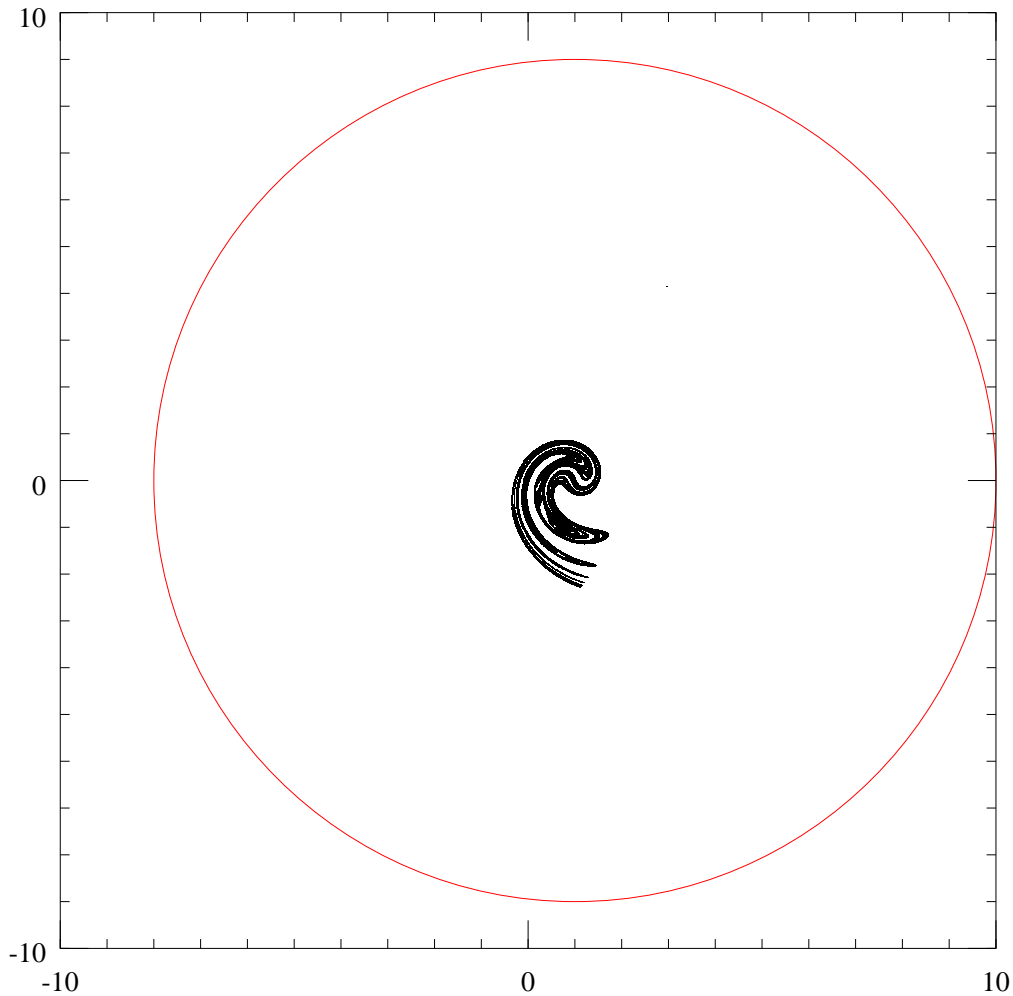


**Figure 5.** Ikeda map,  $\alpha = 6$ , nonwandering part of the trapping region.

### 3.3. Ikeda map for $\alpha = 7$

As a last case we consider a parameter value  $\alpha = 7$ . In simulations one observes convergence of the trajectories to one of the two stable orbits, period-1 orbit and period-2 orbit. This is similar to the first case considered ( $\alpha = 3$ ) where we also observe two stable periodic orbits. As we will see there are many differences between these two cases. In this last case there exists an abundance of periodic orbits and from topological point of view the dynamics is even more complicated than for  $\alpha = 6$  — we observe more unstable periodic orbits, which gives rise to higher topological entropy.

There are three fixed points for the map

$$\begin{aligned} P_1 &\in (3.242600973758_{17}^{21}, 4.284276235174_{27}^{32}), \\ P_2 &\in (0.5419307253256_{16}^{23}, 0.38430085220722_{56}^{96}), \\ P_3 &\in (1.289330937029_{39}^{44}, -2.5780559420601_{57}^{27}). \end{aligned}$$

The first is stable and the two others are unstable. There is one stable period-2 orbit

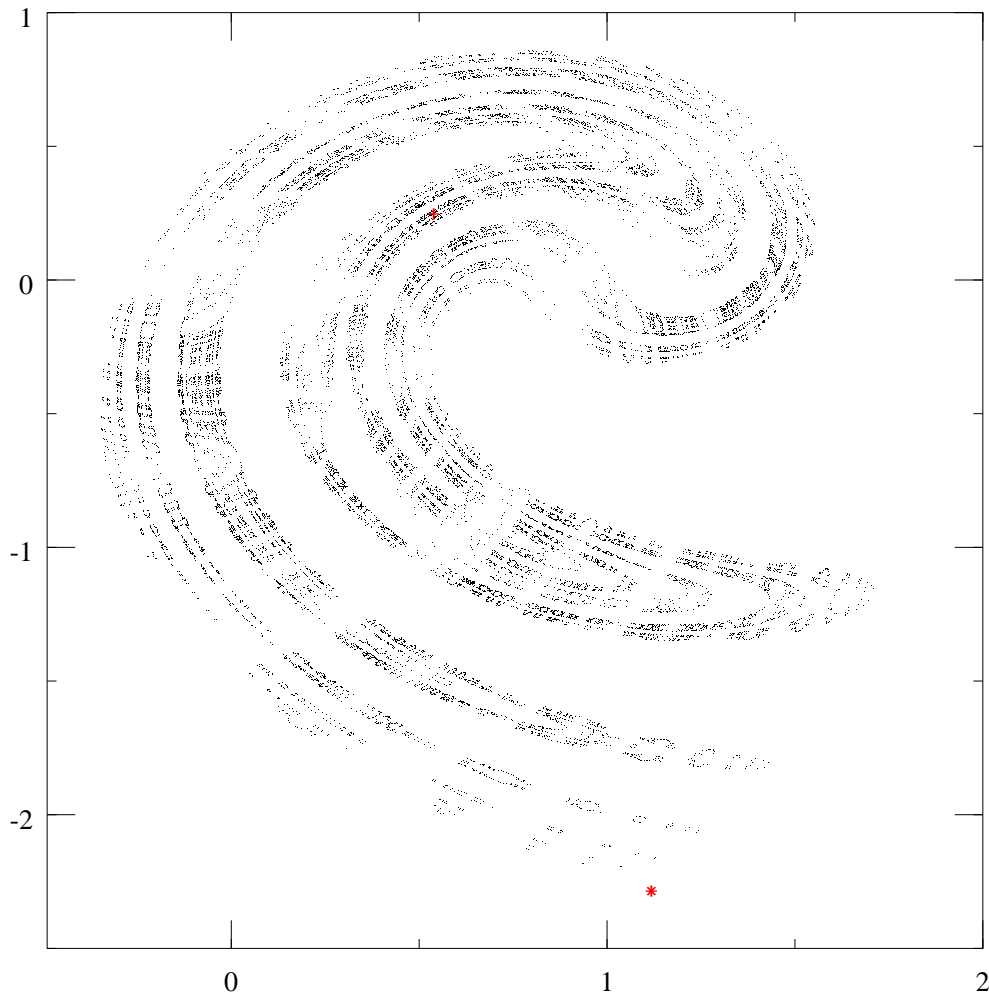


**Figure 6.** Ikeda map,  $\alpha = 6$ , periodic orbits with period  $n = 1, \dots, 15$

$(Q_1, Q_2)$

$$Q_1 \in (1.03884627029997_{25}^{62}, -0.0944284334089_{63}^{53}),$$

$$Q_2 \in (0.0657477429499_{89}^{92}, -0.0924583425239_{58}^{47}).$$

and two unstable period-2 orbits.

As in the previous cases we have found sets containing the invariant part and the nonwandering part of the trapping region. The nonwandering part, which is shown in Fig. 7 consists of three connected regions. Two small regions correspond to the stable fixed point  $P_1$  and the unstable fixed point  $P_3$ . The third region contains stable period-2 orbit and infinitely many unstable periodic orbits. The invariant part contains additionally the unstable manifolds of  $P_3$ . For this parameter value we were able to break the nonwandering region into three parts. This was possible because the unstable fixed point is located further away from the chaotic set. The procedure did not break the large component into two parts. We know however that this in general should be possible. The nonwandering part of the basin of attraction of the stable period-2

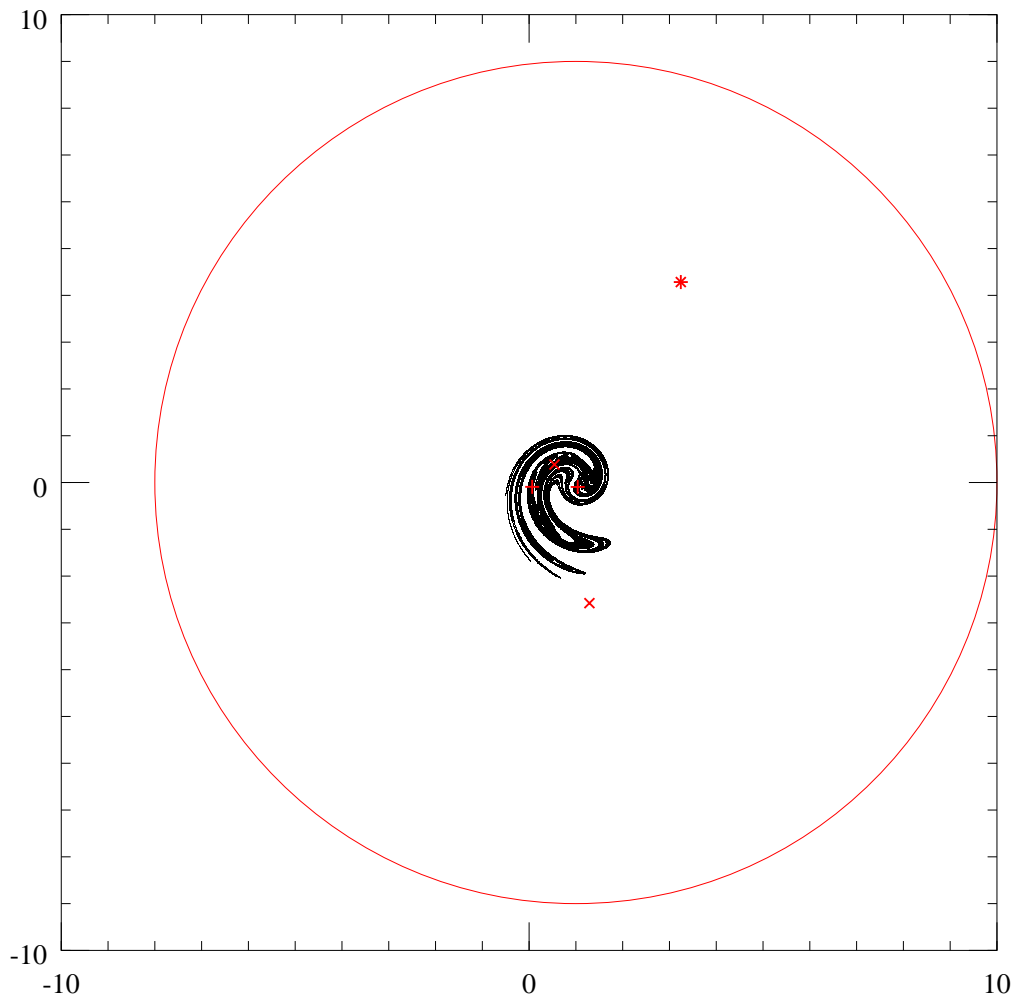


**Figure 7.** Ikeda map,  $\alpha = 7$ , nonwandering part of the trapping region, stable fixed point (\*), unstable fixed points ( $\times$ ), stable period-2 orbit (+)

orbit consists of just two points and this part of the nonwandering set is separated (has nonzero distance) from the chaotic set containing infinitely many unstable periodic orbits.

We have also found the basins of attraction of the stable periodic orbits. They are shown in Fig. 8. The part of the basin of attraction of the stable fixed point found has area of 347.868 within the rectangle  $[-10, 10] \times [-10, 10]$ , while the part of the basin of attraction of the stable period-2 orbit has area of 0.023. This basin of attraction is tangled up with the chaotic set (compare Fig. 9) and it is very difficult to rigorously find the region where it is located.

Finally we have found all cycles with period  $n \leq 12$ . They are plotted in Fig. 9.

### 3.4. Topological entropy

Topological entropy of a map  $f$  is a quantitative measure of its orbit complexity. In topological sense a dynamical system is called chaotic if its topological entropy is

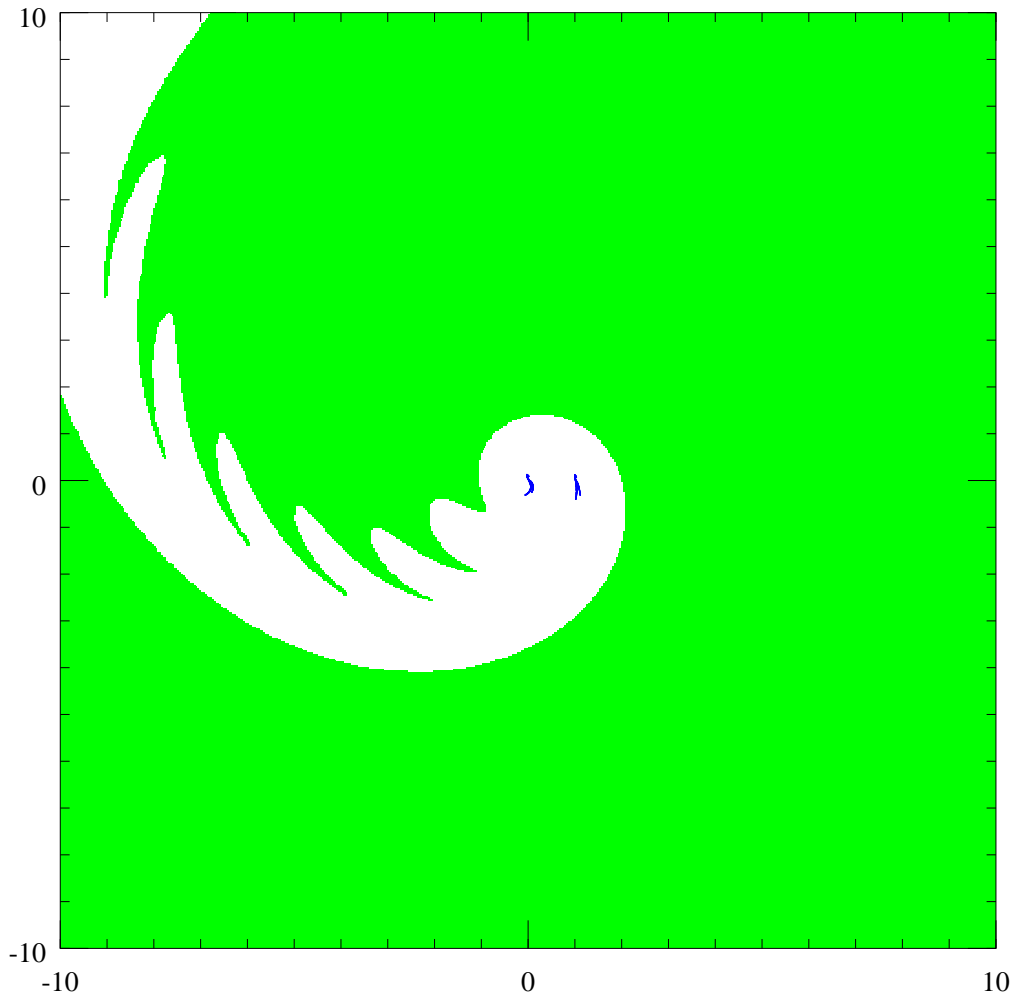


**Figure 8.** Ikeda map,  $\alpha = 7$ , basin of attraction of the stable fixed point and the stable period-2 orbit

positive. Let us recall the definition of topological entropy based on the notion of a separated set. A set  $E$  is called  $(n, \varepsilon)$ -separated if for every two different points  $x, y \in E$ , there exists  $0 \leq j < n$  such that the distance between  $f^j(x)$  and  $f^j(y)$  is greater than  $\varepsilon$ .

Topological entropy of  $f$  is defined as

$$H(f) = \lim_{\varepsilon \rightarrow 0} \limsup_{n \rightarrow \infty} \frac{1}{n} \log s_n(\varepsilon), \quad (9)$$

where  $s_n(\varepsilon)$  is the cardinality of a maximum  $(n, \varepsilon)$ -separated set.

Under certain assumptions (see [3]) the topological entropy can be expressed in terms of the number of periodic orbits

$$H(f) = \limsup_{n \rightarrow \infty} \frac{\log P_n}{n},$$

where  $P_n$  denotes the number of fixed points of  $f^n$ . This formula can be used as the lower bound for the topological entropy as long as the distance between periodic orbits of length  $n$ , which are counted is separated from zero.

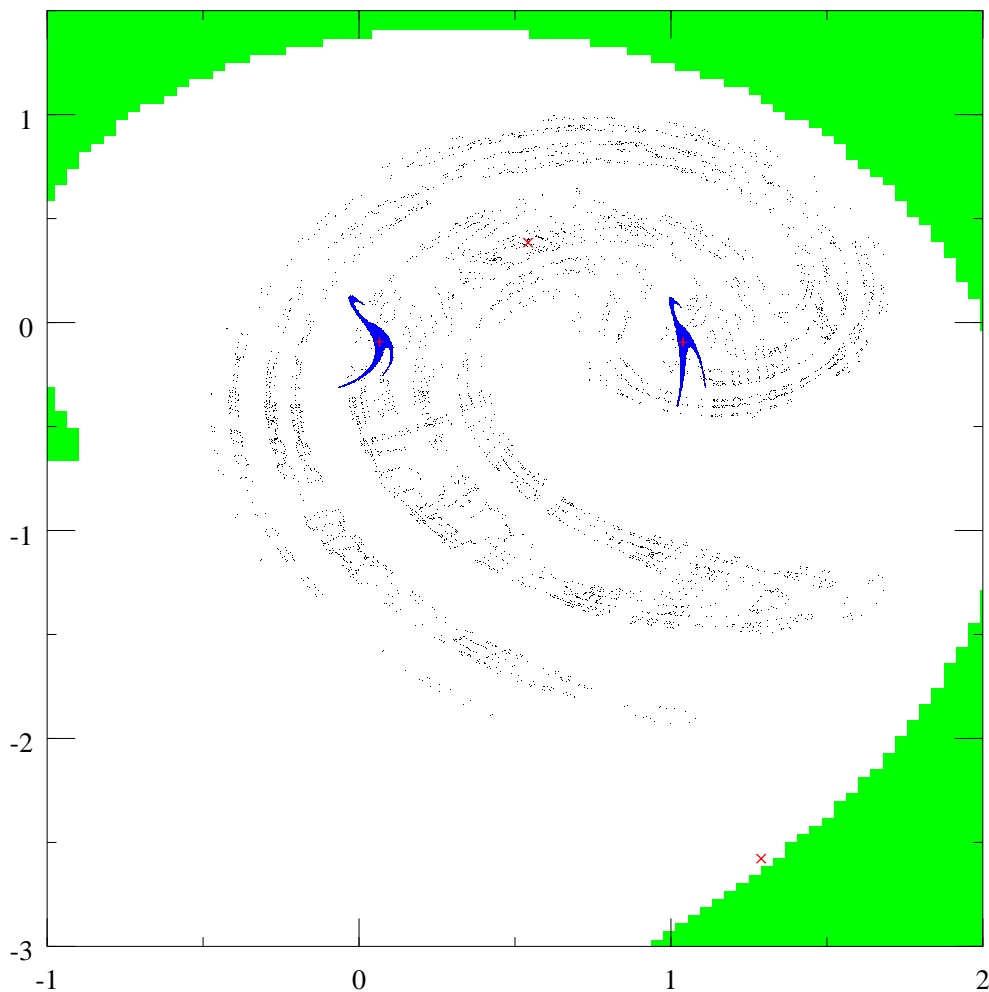


**Figure 9.** Periodic orbit with period  $n \leq 12$  for  $\alpha = 7$ , unstable fixed points ( $\times$ ), stable period-2 orbit ( $+$ ), basin of attraction of the stable fixed point (light), basin of attraction of the stable period-2 orbit (dark).

Hence, it is natural to estimate the topological entropy of the map using the following formula

$$H_n(h) = \frac{\log P_n}{n}.$$

The results on the number of low-period cycles and the estimates  $H_n(h)$  for  $\alpha = 3, 6, 7$  are collected in Table 1 (see also Fig. 10).

For  $\alpha = 3$  there exist only 3 fixed points for the map and there are no other periodic orbits. All trajectories converge to one of the fixed points. It is clear that the topological entropy of the Ikeda map for  $\alpha = 3$  is zero. The approximation of the topological entropy based on the number of fixed points of  $f^n$  approaches 0.

For  $\alpha = 6$  the approximation stabilizes as  $n$  is increased. This lets us state the hypothesis that the topological entropy of the Ikeda map for  $\alpha = 6$  is  $H(f) \approx 0.6$ .

For  $\alpha = 7$  there are more periodic orbits with low period than for  $\alpha = 6$  and hence we obtain higher estimates for the topological entropy (the approximation stabilizes

$n$	$\alpha = 3$			$\alpha = 6$			$\alpha = 7$		
	$Q_n$	$P_n$	$H_n$	$Q_n$	$P_n$	$H_n$	$Q_n$	$P_n$	$H_n$
1	3	3	1.0986	2	2	0.6931	2	2	0.6931
2	0	3	0.5493	1	4	0.6931	3	8	1.0397
3	0	3	0.3662	2	8	0.6931	2	8	0.6931
4	0	3	0.2747	3	16	0.6931	3	20	0.7489
5	0	3	0.2197	4	22	0.6182	4	22	0.6182
6	0	3	0.1831	7	52	0.6585	7	56	0.6709
7	0	3	0.1569	10	72	0.6110	14	100	0.6579
8	0	3	0.1373	14	128	0.6065	20	180	0.6491
9	0	3	0.1221	26	242	0.6099	40	368	0.6565
10	0	3	0.1099	46	484	0.6182	66	688	0.6534
11	0	3	0.0999	76	838	0.6119	104	1146	0.6404
12	0	3	0.0916	110	1384	0.6027	216	2660	0.6572
13	0	3	0.0845	194	2524	0.6026			
14	0	3	0.0785	317	4512	0.6010			
15	0	3	0.0732	566	8518	0.6033			

**Table 1.**  $Q_n$  — number of periodic orbits with period  $n$ ,  $P_n$  — number of fixed points of  $f^n$ ,  $H_n = n^{-1} \log(P_n)$  — estimation of topological entropy.

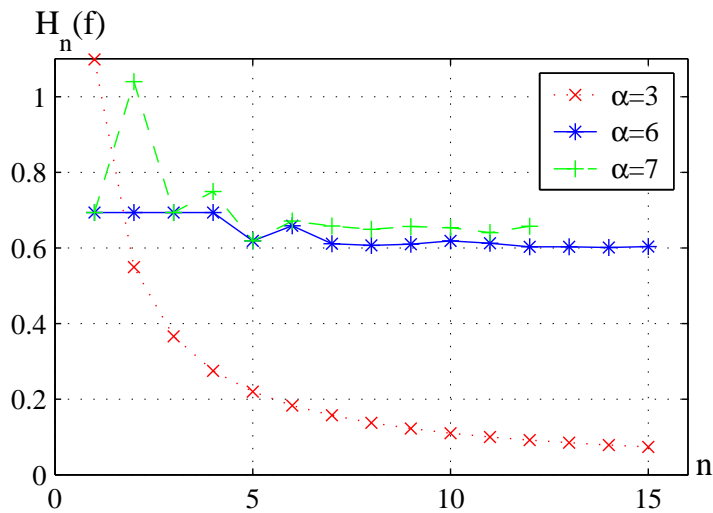


**Figure 10.** Estimation of topological entropy based on the number of low-period cycles

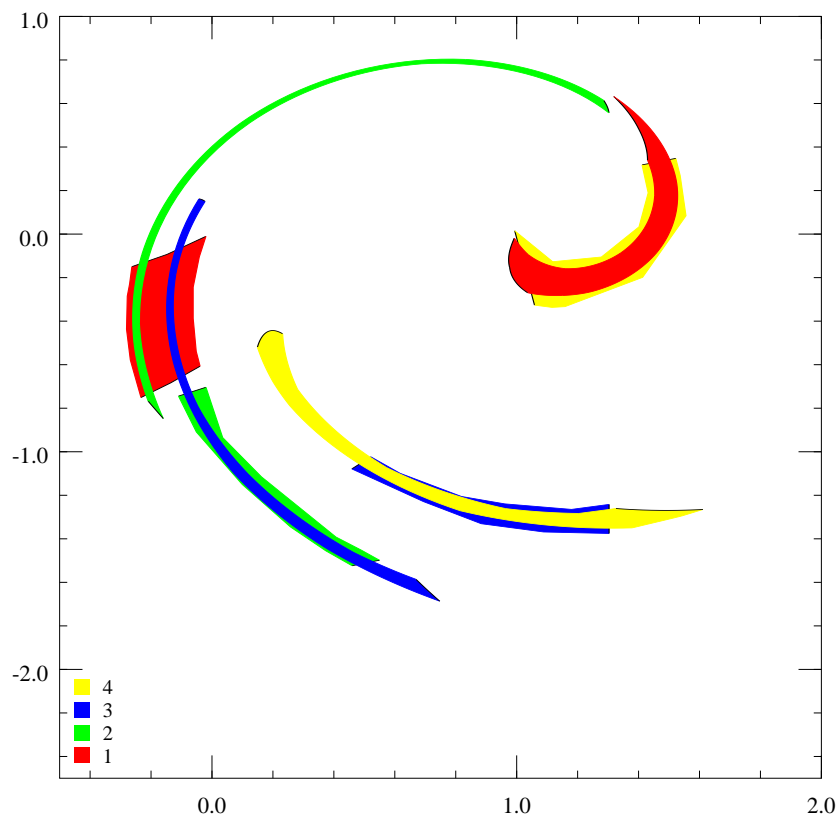


**Figure 11.** Ikeda map,  $\alpha = 6$ , sets  $N_i$  on which the symbolic dynamics on 4 symbols exists and their images

around  $H(f) \approx 0.65$ ). It appears that although in simulations we do not observe complicated behavior the dynamics is more complicated in topological sense than for  $\alpha = 6$ . This complicated dynamics is concentrated on a set which repels trajectories (a chaotic set is a repeller).

### 3.5. Symbolic dynamics

In this section we find symbolic dynamics for the Ikeda map. Since for  $\alpha = 3$  the topological entropy is zero there is no interesting symbolic dynamics for this case. Below we present the analysis for  $\alpha = 6$ . For  $\alpha = 7$  one can use the same technique to prove the existence of symbolic dynamics and to obtain rigorous bounds for topological entropy.

To prove the existence of symbolic dynamics, we first find the nonwandering part of the trapping region. Then we remove boxes for which  $y - x > 1$  or  $y - x < -2$ , and find the invariant part of what is left. This set is then used as an initial guess for the position of rectangles, on which the symbolic dynamics is defined. We modify the position of these rectangles by hand, so that a possibly large number of covering relations hold. The chosen sets and their images under the Ikeda map are shown in Fig. 11. Finally, we check rigorously the existence of covering relations between the chosen sets.

The coverings, the existence of which was proved, correspond to the symbolic

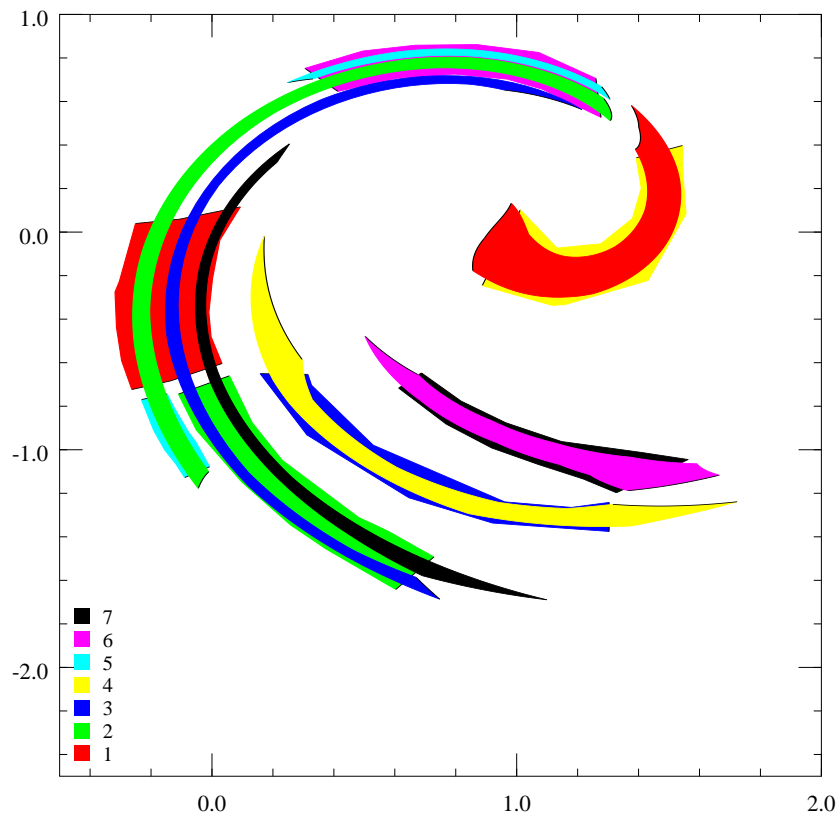


**Figure 12.** Ikeda map,  $\alpha = 6$ , sets  $N_i$  on which the symbolic dynamics on 7 symbols exists and their images

dynamics on four symbols with the following transition matrix:

$$A = \begin{pmatrix} & & & 1 \\ 1 & & & \\ 1 & 1 & & \\ & & & 1 \end{pmatrix}, \quad (10)$$

It follows that the symbolic dynamics with the transition matrix (10) is embedded in  $f$  and that the topological entropy of the Ikeda map is bounded by

$$H(h) > 0.19946.$$

In the second attempt to find the symbolic dynamics we use the same procedure for the finer division of the state space into boxes. This leads to the symbolic dynamics on the seven sets shown in Fig. 12 and the transition matrix

$$A = \begin{pmatrix} & & & & & & 1 \\ 1 & & & & & & \\ 1 & 1 & & & & & \\ & & & & & & 1 \\ & & & & & & 1 \\ 1 & 1 & & & & & \end{pmatrix}. \quad (11)$$



## References

- [1] G. Alefeld. Inclusion Methods for Systems of Nonlinear Equations – The Interval Newton Method and Modifications. In J. Herzberger, editor, *Topics in Validated Computations, Proceedings of the IMACS-GAMM International Workshop on Validated Computation*, pages 7–26. Elsevier, 1994.
- [2] G. Alefeld and J. Herzberger. *Introduction to interval computations*. Academic Press, New York, 1983.
- [3] R. Bowen. Periodic points and measures for axiom A diffeomorphisms. *Trans. Amer. Math. Soc.*, 154:377–397, 1971.
- [4] R.L. Davidchack, Y-C. Lai, A. Klebanoff, and E. Bollt. Towards complete detection of unstable periodic orbits in chaotic systems. *Physics Letters A*, 287:99–104, 2001.
- [5] M. Dellnitz and A. Hohmann. A subdivision algorithm for the computation of unstable manifolds and global attractors. *Numerische Mathematik*, 75:293–317, 1997.
- [6] M. Dellnitz, A. Hohmann, O. Junge, and M. Rumpf. Exploring invariant sets and invariant measures. *Chaos: and Interdisciplinary Journal of Nonlinear Science*, 7(2):221–228, 1997.
- [7] M. Dellnitz, O. Schütze, and S. Sertl. Finding zeros by multilevel subdivision techniques. *IMA Journal of Numerical Analysis*, 22(2):167–185, 2002.
- [8] G. Froyland, O. Junge, and G. Ochs. Rigorous computation of topological entropy with respect to a finite partition. *Physica D*, 154:68–84, 2001.
- [9] Z. Galias and P. Zgliczyński. Abundance of homoclinic and heteroclinic orbits and rigorous bounds for the topological entropy for the Hénon map. *Nonlinearity*, 14:909–932, 2001.
- [10] A. Gibbons. *Algorithmic graph theory*. Cambridge University Press, Cambridge, 1985.
- [11] S.M. Hammel, C.K.R.T. Jones, and J.V. Moloney. Global dynamical behavior of the optical field in a ring cavity. *J. Opt. Soc. Am. B*, 2(4):552–564, 1985.
- [12] C.S. Hsu. Global analysis by cell mapping. *Int. J. Bifurcation and Chaos*, 4(2):727–771, 1992.
- [13] R.B. Kearfott and M. Novoa. Algorithm 681: INTBIS, a portable interval Newton/bisection package. *ACM Trans. Math. Software*, 16(2):152–157, 1990.
- [14] R.E. Moore. *Methods and applications of interval analysis*. SIAM, Philadelphia, 1979.
- [15] A. Neumaier. *Interval methods for systems of equations*. Cambridge University Press, 1990.
- [16] S. Newhouse and T. Pignataro. On the estimation of topological entropy. *Journal of Statistical Physics*, 72:1331–1351, 1993.
- [17] G. Osipenko. Symbolic analysis of the chain recurrent trajectories of dynamical systems. *Differential Equations and Control Processes*, 4, 1998.
- [18] C. Robinson. *Dynamical Systems: Stability, Symbolic Dynamics, and Chaos*. CRC Press, USA, 1995.
- [19] A. Szymczak. A combinatorial procedure for finding isolating neighborhoods and index pairs. *Proc. Royal Society of Edinburgh*, 127A:1075–1088, 1997.
- [20] P. Zgliczyński. Computer assisted proof of chaos in the Rössler equations and the Hénon map. *Nonlinearity*, 10(1):243–252, 1997.